High-Res Gamma Ray Multiplier Tubes (HGMTs) Based on Surface Direct Conversion in Laminar MCPs

Cameron Poe[1], Kepler Domurat-Sousa[1], Peter Scheidt[1], Ian Goldberg[1], Henry Frisch[1], Camden Ertley[2], Neal Sullivan[3]

[1]Enrico Fermi Institute, University of Chicago, [2]Southwest Research Institute, [3]Angstrom Research, Inc.

Introduction

The high-resolution gamma ray multiplier tube (HGMT™) is a gamma ray detector that does not use a scintillator or photocathode [1]. Built out of laminar microchannel plates (LMCPs™), gamma rays interact near a microchannel pore via the photoelectric or Compton effects to produce electrons that can penetrate the pore and start a secondary electron cascade; this process is termed surface direct conversion (SDC) [2]. The HGMT is a vacuum package of a converter LMCP, amplifier LMCP, and an anode. HGMTs are large-area devices with high spatial and time resolutions with applications in TOF-PET, which is covered in this poster. Other applications may include shower-max detectors or searches for rare kaon decays.

LMCPs

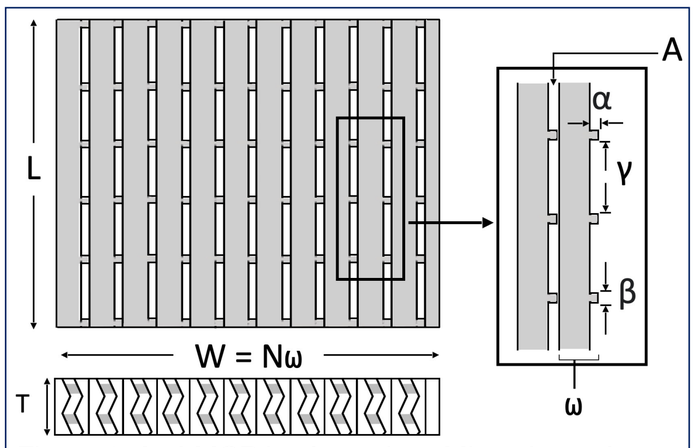

Figure 1: An LMCP in plane view. Microchannels are formed by stacking back-to-back patterned laminae.

The laminar microchannel plate (LMCP) is a type of microchannel plate manufactured by stacking thin, patterned laminae. Patterned laminae can be formed by subtractive methods like machining or etching, additive methods such as 3D printing, or by stamping. Features in the tens of microns are not formed via heating and drawing, so more types of substrate material may be used. Having access to the pores before forming the MCP slab allows for non-conventional coating deposition methods, such as CVD diamond. Unique voltage configurations and surfaces can be patterned in a pore as well as complex channel geometries, such as incorporating an ion feedback-reducing chevron directly into a single MCP slab. Fig. 1 shows zig-zags in the pore, one possible complex geometry.

Surface Direct Conversion

LMCPs packaged into HGMTs can detect gamma rays via the process of surface direct conversion (SDC): When a gamma ray interacts via the Compton or photoelectric effect near the surface of a substrate, and the resulting electron has sufficient energy, the electron can escape the substrate surface. Due to the high surface-area to volume ratio of an LMCP, SDC has a high conversion efficiency (defined to be number of gammas that produce an primary electron that escapes into a pore). Geant4 simulations are used to find the optimal LMCP geometries for a given material where conversion efficiency is maximized. Figs. 2 and 3 present these Geant4 simulations.

Geometry Optimization

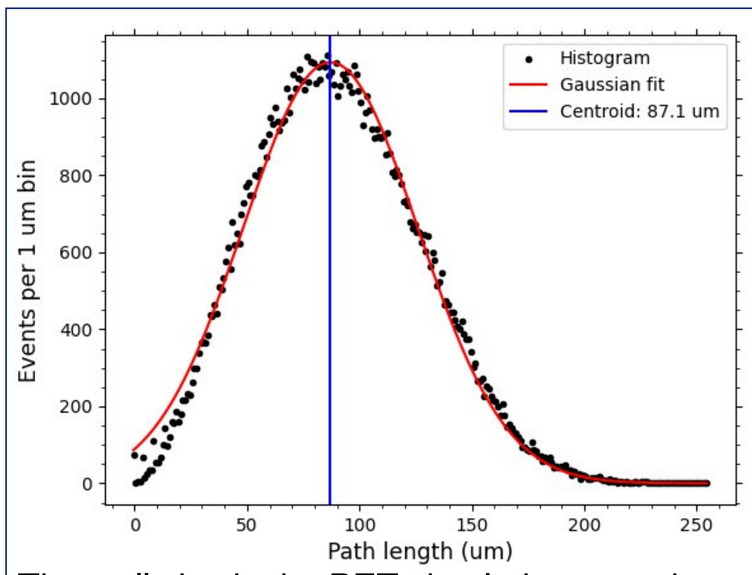

Fig 2: Histogram of path length for 400 keV electrons traveling in NIST Pb-glass. Although not a perfect Gaussian distribution, the centroid of ~90 um is obtained from a Gaussian fit to the data.

The wall size in the PET simulation was chosen as 50 um from simulations of mean distance traveled of electrons in NIST Pb-glass [4]. In a high-Z substrate, the photoelectric effect dominates, and 511 keV gamma rays will produce ~400 keV electrons (gamma energy minus K-shell binding energy). A Geant4 simulation tracked the distance from where the electron started and the location where it deposits the last of its energy. Fig. 2 shows the mean path length is ~90 um, so feature size should be on the order of tens of um.

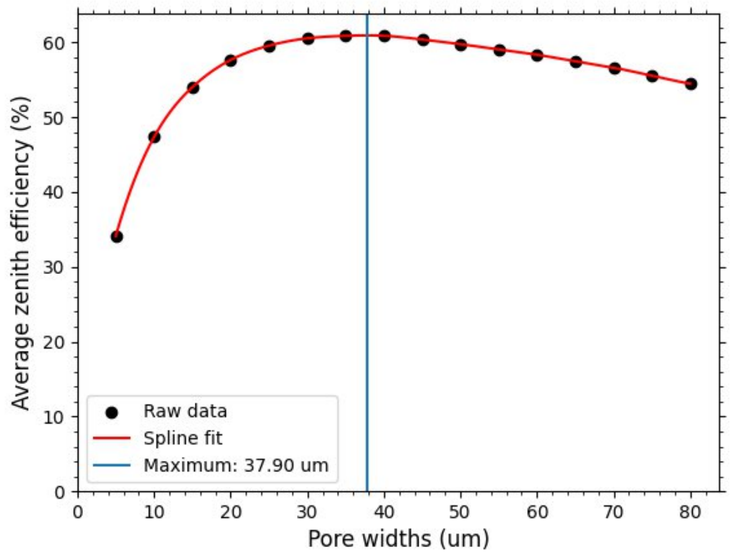

Fig 3: Pore width optimization in Geant4 for a 1 in-thick LMCP with 50 um square pores. Average zenith efficiency is averaged conversion efficiency (fraction of events with a primary electron entering pore) averaged over gamma ray angles of incidence.

The optimal pore width of the HGMT was 50 um for square pores and a wall thickness of 50 um. Fig. 3 shows a Geant4 simulation swept over a range of pore widths and calculated the average conversion efficiency for a variety of angles of incidence. The shallow slope near the maximum can be exploited based on different manufacturing techniques. 3D printing can use a larger pore width such as 75 um to speed up print times without sacrificing much efficiency, while a subtractive method like laser etching may benefit from smaller pores closer to 25 um.

TOF-PET Simulation

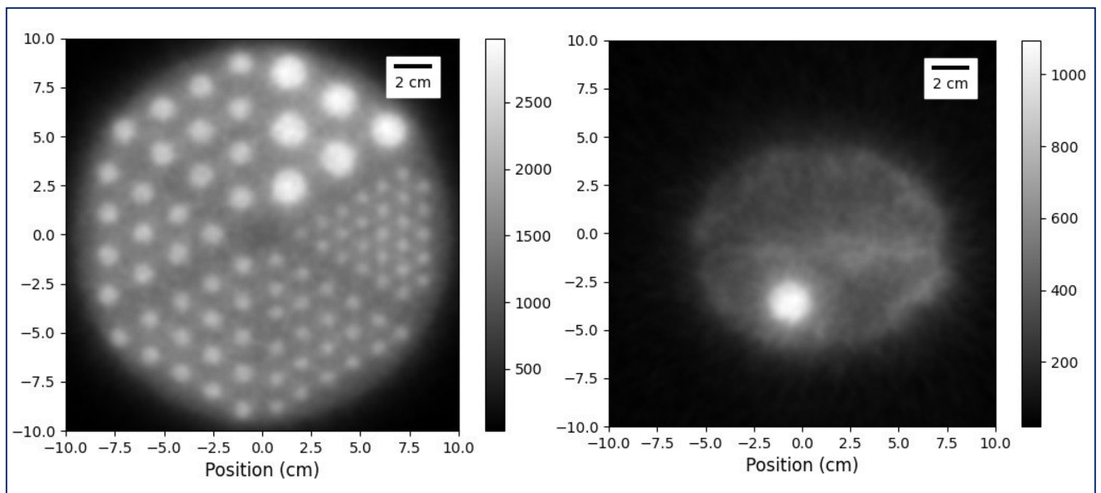

Fig 4: Left: the Derenzo phantom at 1/100th dose compared to a baseline scan of 10 minutes at 5 kBq/mL background and 15 kBq/mL hot rods. Right: the XCAT computational brain phantom at 1/100th dose compared to a baseline scan of 10 minutes at 8.25 kBq/mL in the white matter, 33 kBq/mL in the gray matter, and 99 kBq/mL in the 2 cm diameter lesion [7]. Both phantoms were imaged in a TOPAS simulation of a 2 m long scanner with HGMTs of 2.54 cm converter thickness and 50 um pore size and wall thickness, with 100 ps FWHM time resolution and 1 mm sigma spatial resolution. Reconstruction was directly summed the lines-of-response.

Fig. 4 shows 1/100th dose scans of the Derenzo and XCAT brain phantoms [4, 5] using a total-body (2 m long) HGMT scanner simulated in TOPAS [6]. TOPAS is a wrapper for Geant4 that provides a simplified user interface and straightforward compatibility with phantoms for medical imaging, such as the XCAT phantom used in this simulation. The HGMT was parameterized with the efficiencies of the Geant4 simulation as well as given time resolution of 100 ps FWHM and spatial resolution of 1 mm sigma. The smallest rod of the Derenzo (r = 3.2 mm) and the lesion in the brain phantom are both clearly visible at low dose.

Test Stand

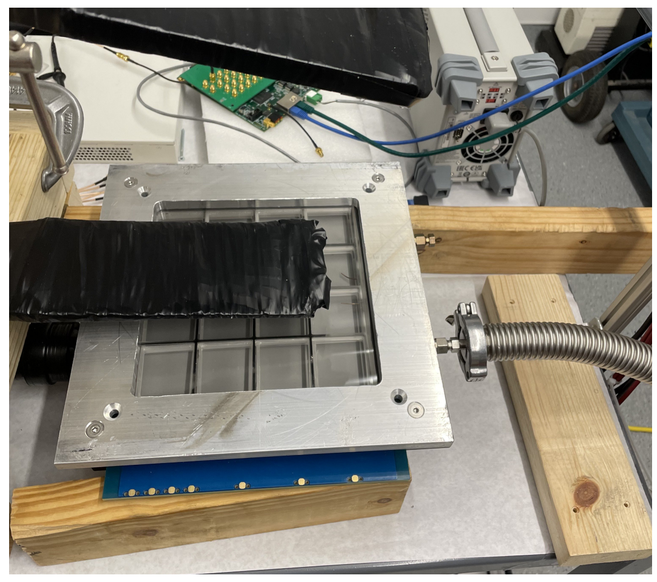

Fig 5: The current UofC LMCP test stand.

To test the conversion and amplification properties of the LMCP, we are building an LMCP test stand at the University of Chicago. Fig. 5 shows the current progress. The LMCP will be housed in a ceramic tile-base with a removable window capable of housing beta and gamma button sources. Vacuum is generated by a Pfieffer leak detector. The tile-base has a NiCr baseplate capacitively coupled to a strip-line pickup board read out with PSEC4 electronics in a similar method to current LAPPDs. PSEC4 has been shown to have a time resolution of 3.22 ps [8]. A PMT cosmic ray test stand will help calibrate the electronics and calculate conversion efficiencies.

Summary and Next Steps

TOPAS and Geant4 simulations show that HGMTs can detect gamma rays and be used for TOF-PET at a dose reductions of 1/100th. This is ideal for expanding into rural and under-served regions lacking access to PET scanners.

The next steps for the simulation are to investigate the difference between high-Z and low-Z converter LMCPs in HGMTs to see if some in-patient scatter rejection can be incorporated into the reconstruction.

While the test stand is being finished, we are talking with multiple vendors about how to pattern or even 3D print laminae, as well as see what types of nonconventional substrates can be used in LMCPs.

Acknowledgments

We thank Joseph Perl and Paul Segars for the exemplary development of TOPAS and XCAT and for their remarkable user support. We are indebted to Mary Heintz for exceptional computational system development and advice. Benjamin Cox provided highly informed encouragement, advice, and support. K. Domurat-Sousa, and C. Poe were supported by the University of Chicago College, Physical Sciences Division, and Enrico Fermi Institute, for which we thank Steven Balla and Nichole Fazio, Michael Grosse, and Scott Wakely, respectively. C. Poe was additionally supported by the University of Chicago Quad Undergraduate Research Scholars program and the Jeff Metcalf Internship program.

References

[1] K. Domurat-Sousa, et al. Nucl. Instrum. Methods, 1057:168676, 2023
[2] K. Domurat-Sousa, et al. Nucl. Instrum. Methods, 1055:168538, 2023
[3] NIST lead glass. https://web.archive.org/web/20230629203158/https://physics.nist.gov/cgi-bin/Star/compos.pl?matno=170. Accessed: 2023-10-09
[4] S. Derenzo, et al. IEEE Trans Nucl Sci. 1977;24(1):544-558. doi:10.1109/TNS.1977.4328738
[5] W. Segars, et al. Med Phys. 2010;37(9):4902-4915. doi:10.1118/1.3480985
[6] B. Faddegon, et al. Phys Med, 72:114–121, Apr 2020
[7] J. Lee, et al. Surg Neurol Int. 2011;2(1):158. doi:10.4103/2152-7806.89857
[8] J. Pastika, FTBF Time of Flight Upgrade, CPAD 2023.